

## Event-Related Potential, Time-frequency, and Functional Connectivity Facets of Local and Global Auditory Novelty Processing: An Intracranial Study in Humans

Imen El Karoui<sup>1</sup>, Jean-Remi King<sup>1,2,3</sup>, Jacobo Sitt<sup>1,2,3</sup>, Florent Meyniel<sup>1</sup>, Simon Van Gaal<sup>1,2,3</sup>, Dominique Hasboun<sup>1,4</sup>, Claude Adam<sup>5</sup>, Vincent Navarro<sup>1,2,5</sup>, Michel Baulac<sup>5</sup>, Stanislas Dehaene<sup>2,3,6,7</sup>, Laurent Cohen<sup>1,5</sup> and Lionel Naccache<sup>1,4,5</sup>

<sup>1</sup>INSERM U1127, CNRS UMR 7225, Sorbonne Universités, UPMC Univ Paris 06, UMR S 1127, Institut du Cerveau et de la Moelle épinière, ICM, Equipe PICNIC Paris 75013, France, <sup>2</sup>Cognitive Neuroimaging Unit, INSERM U992, Gif-sur-Yvette 91191, France, <sup>3</sup>NeuroSpin Center, Institute of BioImaging, Commissariat à l'Energie Atomique, Gif-sur-Yvette 91191, France, <sup>4</sup>AP-HP, Groupe Hospitalier Pitié-Salpêtrière, Department of Neurophysiology, Paris 75013, France, <sup>5</sup>AP-HP, Groupe Hospitalier Pitié-Salpêtrière, Department of Neurology, Paris 75013, France, <sup>6</sup>Université Paris 11, Orsay 91400, France and <sup>7</sup>Collège de France, Paris 75005, France

Address correspondence to Imen El Karoui, Email: imen.elkaroui@gmail.com; Lionel Naccache, Email: lionel.naccache@gmail.com

**Auditory novelty detection has been associated with different cognitive processes. Bekinschtein et al. (2009) developed an experimental paradigm to dissociate these processes, using local and global novelty, which were associated, respectively, with automatic versus strategic perceptual processing. They have mostly been studied using event-related potentials (ERPs), but local spiking activity as indexed by gamma (60–120 Hz) power and interactions between brain regions as indexed by modulations in beta-band (13–25 Hz) power and functional connectivity have not been explored. We thus recorded 9 epileptic patients with intracranial electrodes to compare the precise dynamics of the responses to local and global novelty. Local novelty triggered an early response observed as an intracranial mismatch negativity (MMN) contemporary with a strong power increase in the gamma band and an increase in connectivity in the beta band. Importantly, all these responses were strictly confined to the temporal auditory cortex. In contrast, global novelty gave rise to a late ERP response distributed across brain areas, contemporary with a sustained power decrease in the beta band (13–25 Hz) and an increase in connectivity in the alpha band (8–13 Hz) within the frontal lobe. We discuss these multi-facet signatures in terms of conscious access to perceptual information.**

**Keywords:** connectivity, intracranial recordings, mismatch negativity, P300, time-frequency

### Introduction

Novelty detection is fundamental to quickly respond to potentially relevant stimuli. It is notably important to detect both unusual objects (perceptual novelty) and usual objects delivered in a new context. This second type of novelty, termed “contextual novelty,” has been widely studied using ERPs. Two main cognitive processes, a fast and automatic novelty detection process and a slow and strategic one, have been identified. The first one is indexed by the mismatch negativity (MMN—Näätänen et al. 1978), which is elicited around 100–200 ms after change onset. The MMN is generated by bilateral sources in the superior temporal cortex and possibly in the frontal cortex (Giard et al. 1990; Rinne et al. 2000; Opitz et al. 2002). These generators were confirmed by intracranial studies conducted in humans (Halgren et al. 1995; Kropotov et al. 2000; Liasis et al. 2001; Rosburg et al. 2005). Interestingly, the MMN persists in the absence of attention (Näätänen et al. 1978). It can even be observed during rapid eye-movement sleep (Atienza et al. 1997) or in comatose patients (Fischer et al.

1999; Naccache et al. 2005) or more generally in patients with impaired consciousness (Faugeras et al. 2011, 2012; King et al. 2013). Following the MMN, another component sensitive to auditory novelty, the P300, can be recorded about 300 ms after change onset (Sutton et al. 1965) and is related to a strategic novelty detection process. Two types of P300 can be distinguished. The P3a is anteriorly distributed, peaks between 220 and 280 ms, and is weakly affected by attention (Squires et al. 1975), whereas the P3b is a centro-posterior component, reflecting the activation of the hippocampus and parietal and frontal cortices (Picton 1992), and spanning from 250 to 600 ms after change onset. The P3b is highly dependent on attention, as it only occurs when subjects are actively engaged in detecting novel stimuli (Bekinschtein et al. 2009). Therefore, it has been proposed as a neural signature of working memory (Donchin and Coles 1988; Polich 2007) and conscious access (Sergent et al. 2005).

Bekinschtein et al. (2009) developed an experimental paradigm exploring these 2 processes. It relies on 2 levels of auditory novelty that are orthogonally manipulated: a change in pitch within series of 5 sounds (local novelty) gives rise to an MMN, whereas a rare change in series of 5 sounds in a fixed context (global novelty) triggers a P3b. An fMRI experiment using this exact paradigm showed that local novelty elicited responses within auditory cortices, whereas processing of global novelty was associated with a distributed brain network including frontal, anterior cingulate, and parietal areas (Bekinschtein et al. 2009). Interestingly, the response to local novelty was present even when subjects were distracted, whereas the response to global novelty only occurs when subjects were actively engaged in detecting novel stimuli (Bekinschtein et al. 2009) or when they were paying attention to the stimuli (Wacongne et al. 2011). Moreover, using this paradigm, responses to local novelty were observed in patients with impaired consciousness, but responses to global novelty were only observed in patients with preserved consciousness (Faugeras et al. 2011, 2012; King et al. 2013).

Taken together, these findings suggest that local novelty detection involves a fast, automatic, and encapsulated process, whereas global novelty detection involves a slow, strategic, and widespread process.

Nevertheless, responses to local and global novelty have mostly been explored using ERP measures, but it is important to explore their oscillatory properties and functional connectivity in order to fully understand the networks underlying these

2 types of responses, as evidenced in previous intracranial studies (Axmacher et al. 2010; Zaehle et al. 2013). Indeed, responses to events of interest contain modulations in some frequency bands that are time-locked to the events, but not phase-locked, and thus cannot be extracted by ERPs (Pfurtscheller and Lopes da Silva 1999; Tallon-Baudry and Bertrand 1999). In particular, modulations in high gamma activity has been proposed to reflect local spiking activity (Pesaran et al. 2002; Nir et al. 2007; Ray and Maunsell 2010), which cannot be measured by ERPs. Moreover, interactions between brain regions cannot be explored by ERPs but are thought to be reflected in modulations of power in the beta band (Kopell et al. 2000) and in functional connectivity measures, such as phase coupling (Fries 2005).

We thus compared spatio-temporal dynamics of the responses to local and global novelty by analyzing ERPs, spectral power, and functional connectivity, in 9 epileptic patients with intracranial electrodes, taking advantage of the high spatial and temporal resolutions of these recordings.

We predicted responses to local novelty to be confined within superior temporal cortices and to appear as an intracranial MMN ERP, contemporary with an increase in gamma-band power indexing localized neural activity (Pesaran et al. 2002) and associated with no clear increase in long-range functional connectivity. In sharp contrast, we predicted responses to global novelty to be more widespread across brain regions, including in particular parietal and frontal areas: indeed global novelty detection involves working memory, and frontoparietal areas have been associated with this effect in MEG (Wacongne et al. 2011) and fMRI (Bekinschtein et al. 2009) studies. We also predict that these responses should appear as a maintained ERP peaking around 300 ms, contemporary with a modulation in beta-band power, which has been associated with long-range communication (Donner and Siegel 2011), and with direct evidence of inter-area connectivity.

## Materials and Methods

### Patients

Ten epileptic patients (age  $M=32$  years old,  $SD=11$  years; 4 males—see Table 1) gave their written informed consent to participate in this study. Neuropsychological assessment revealed normal or mildly impaired general cognitive functioning (IQ ranged from 77 to 98) for all patients but one. This last patient had an extremely low IQ of 64 but was able to do the task properly (97% accuracy). These patients suffered from drug-refractory focal epilepsy and were implanted stereotactically with depth electrodes as part of a presurgical evaluation. Implantation sites were selected on purely clinical criteria, with no reference to the present protocol. This experiment was approved by the

ethical committee of Pitié-Salpêtrière Hospital (Comité Consultatif de Protection des Personnes participant à une Recherche Biomédicale). Based on poor behavioral performance (only 56% accuracy), Patient 10 was excluded.

### Procedure

The procedure used in this experiment exactly followed the “Local-Global” paradigm, developed by Bekinschtein et al. (2009), who already reported intracranial ERPs from 2 of the present patients.

Patients were presented with 8 blocks of 123–128 trials. In each trial, a series of 5 sounds were played over a total of 650 ms. The first 4 sounds were always identical, either low- (sound A) or high-pitched (sound B), but the fifth one could be either identical (AAAAA orBBBBB) or different (AAAAB orBBBBBA). Thus, this last sound respects or violates the local regularity established by the first 4 sounds in local standard or local deviant trials, respectively (Fig. 1). On top of this local rule, a global regularity was added. In each block, global standard trials were delivered on 80% of trials. In the first type of blocks, these trials were local standard trials, whereas in the second type of blocks, they were local deviant trials. In contrast, global deviant trials were presented in 20% of trials in a given block (Fig. 1). In the first type of blocks, these trials were local deviant trials, whereas in the second type of blocks, they were local standard trials. The first 20–30 trials of each block were global standard trials to establish the global regularity.

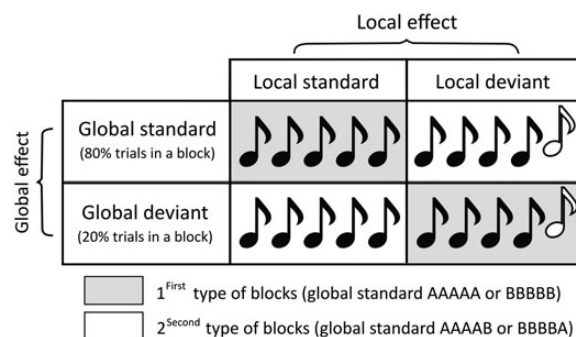


**Figure 1.** The Local Global paradigm. The Local Global paradigm (Bekinschtein et al. 2009) is an auditory oddball paradigm with 2 levels of regularity. Each trial is composed of a series of 5 successive sounds (SOA = 150 ms). The first 4 sounds are always identical. The fifth sound can either be identical to these first sounds in local standard trials or different in local deviant trials. On top of this local regularity, a global rule is added. Global deviant trials correspond to a series of 5 sounds, which is rare in a given block, compared with the frequent global standard trials. Local and global regularities are manipulated orthogonally, resulting in 4 types of trials: local standard-global standard and local deviant-global deviant in the first type of blocks, and local deviant-global standard and local standard-global deviant in the second type of blocks. Two sounds were used to generate these trials: sound A (composed of 350-, 700-, and 1400-Hz sinusoidal tones) and sound B (composed of 500-, 1000-, and 2000-Hz sinusoidal tones). The local effect corresponds to the difference between local deviant and local standard stimuli, whereas the global effect corresponds to the difference between global deviant and global standard stimuli.

**Table 1**  
Clinical characteristics of the patient sample

Patient	Age	Gender	Handedness	Epilepsy duration (year)	Total number of electrodes	Temporal electrodes	Frontal electrodes	Occipital electrodes
1	18	F	R	8	36	36	0	0
2	29	F	R	4	25	25	0	0
3	48	F	L	10	37	37	0	0
4	46	F	R	25	14	11	3	0
5	23	M	R	8	43	10	33	0
6	43	F	R	24	27	11	16	0
7	26	M	L	16	42	40	0	2
8	42	M	R	26	9	0	9	0
9	26	M	R	11	49	24	0	25
10	24	F	R	14	72	9	63	0

Note: Patient 10 was excluded from the analysis as she did not perform the task correctly (56% accuracy).

Local and global regularities were thus manipulated orthogonally (Fig. 1). This design enables the comparison between physically identical stimuli in different contexts. In the following analyses, we will refer to local and global effects, which correspond respectively to the contrast between local deviant versus local standard stimuli, and between global deviant versus global standard stimuli (Fig. 1). Additionally, patients were instructed to actively count the number of global deviant trials and report this number at the end of each block. This task ensured that they were paying attention to the stimuli.

Each sound was 50-ms long and composed of 3 sinusoidal tones (350, 700, and 1400 Hz, sound A; or 500, 1000, and 2000 Hz, sound B). All tones were prepared with 7-ms rise and 7-ms fall times. Four different series were used: AAAAA, BBBB, AAAAB, and BBBBA. The stimulus onset asynchrony (SOA) between sounds was 150 ms. A series of sounds were separated by a variable silent interval of 1350–1650 ms. Four different blocks were thus created, with each possible series of sounds as global standard trials. All patients heard each of these blocks twice, in randomized order. Sounds were presented from the computer's speakers, using E-prime v1.2 (Psychology Software Tools, Inc.) at the bedside of each patient.

### Electrode Implantation and Localization

Patients were implanted intracerebrally with depth electrodes, each bearing 4–10 recording sites (Ad-TechMedical Instruments). Each patient had on average 59 (SD = 13) recording sites.

To compare position of recording sites and summarize brain activations across patients, their coordinates were obtained after normalizing the anatomical three-dimensional post-implantation MRI onto the template from the Montreal Neurological Institute, using SPM8 software (<http://www.fil.ion.ucl.ac.uk/spm>). Electrodes localization plots used the iso2mesh toolbox (Fang and Boas 2009; Fang 2010).

### Data Acquisition and Preprocessing

For 7 patients, data were acquired with an audio–video–EEG monitoring system (Micromed), which allowed for simultaneous acquisition of data from up to 128 EEG channels sampled at 1024 Hz. Data from the remaining 3 patients were acquired using another audio–video–EEG monitoring system (Nicolet-Viasys), which allowed for simultaneous acquisition of data from up to 64 EEG channels sampled at 400 Hz.

Unless specified otherwise, data were analyzed with Fieldtrip toolbox (Oostenveld et al. 2011) and Matlab 2011a (The Mathworks, Inc.). All the analyses were done at the electrode level, as the position of the recording sites differed from one patient to another.

Epochs were extracted (from –800 to 700 ms after the onset of the fifth sound). To avoid artifacts, recording sites exceeding the threshold of  $\pm 300$   $\mu$ V in more than 5% of the epochs were excluded. All signals were re-referenced to their nearest neighbor on the same electrode (bipolar montage). In the following, we will refer to these bipolar montages as “electrodes.” All data were visually inspected to discard any trial with epileptic activity.

### Behavioral Analysis

Patients were instructed to count silently the number of global deviants and report this number. For each patient, we computed the average percentage of errors over blocks and we report accuracy as 100% minus this percentage.

### ERP Analysis

Event-related potentials (ERPs) were obtained by averaging epochs for each condition. The signal was band-pass filtered off-line from 0.5 to 20 Hz using a fourth-order Butterworth filter in forward and reverse directions in order to avoid phase-shift, and a baseline correction was applied, by subtracting the mean voltage in the [–800 ms 0 ms] window.

To assess the statistical significance of our results, ERPs of local deviant trials and global deviant trials were compared with those of local standard trials and global standard trials, respectively, using independent sample *t*-tests for each electrode. To control for type I errors

generated by multiple comparisons across time at level  $\alpha$ , we used a nonparametric procedure. We computed  $N = 1000$  permutations by shuffling trial labels. For each permutation, the maximal *t*-value across time samples was extracted to estimate the permutation distribution of the maximal statistic. The critical threshold that controls for family-wise error rate over time samples was defined as the  $c + 1$  largest member of this distribution, where  $c$  is equal to  $\alpha N$  rounded down. In the original data, only samples with a *t*-value higher than this threshold were identified as significant (Nichols and Holmes 2002). In addition, to correct for multiple comparison over electrodes when visualizing effects across all electrodes in all patients, we used a false discovery rate (FDR) correction on *P*-value obtained at the electrode level, across the whole time window. All reported *P*-values are corrected and referred to as  $P_{\text{corr}}$ .

Peak latencies were identified within periods of statistical significance on the difference between standard and deviant trials. For the sustained responses to global novelty, latencies were estimated as the earliest significant differences given the absence of a clear peak. In both cases, reported latencies are the average across all significant electrodes.

### Time-Frequency Analysis

Time-frequency representations were calculated by Morlet wavelets, as described previously (Tallon-Baudry et al. 1997). The power at a given time *t* and frequency  $f_0$  is given by the squared norm of the convolution of the signal to the wavelet  $w(t, f_0)$ :

$$w(t, f_0) = A \exp\left(\frac{-t^2}{2\sigma_t^2}\right) \exp(2i\pi f_0 t) \quad \text{where } A = (\sigma_t \sqrt{\pi})^{-1/2}.$$

The width of the wavelet  $m = 2\pi\sigma_t f_0$  was set to 5 as this value gives a good tradeoff between time and frequency resolution (De Moortel et al. 2004). The length of each wavelet used for the computation was  $3\sigma_t$ . The convolution of the signal by this set of wavelets resulted in an estimate of power at each time sample and at each frequency (2-Hz step) between 5 and 200 Hz. Power was then converted to a decibel (dB) scale. Time-frequency values were obtained from the subtraction between 2 conditions, without baseline correction.

To assess the significance of differences in oscillation power across conditions, we used independent sample *t*-tests at each time and frequency point. Then, correction for multiple comparisons over time and frequency was performed, by nonparametric cluster-based method (Maris and Oostenveld 2007). We computed  $N = 1000$  permutations by shuffling trial labels. Then, for each permutation, independent sample *t*-tests were performed at each time and frequency sample. All samples with a *t*-value corresponding to a *P*-value smaller than 0.05 were clustered in connected sets on the basis of adjacency in time and frequency. Then, the cluster statistic was computed by taking the sum of the *t*-values within each cluster. The cluster-corrected threshold was obtained by computing the permutation distribution of the maximum cluster statistic and taking the  $c + 1$  largest member of this distribution, with  $c$  is equal to  $\alpha N$  rounded down. In the original data, only clusters with a cluster statistic higher than this threshold were identified as significant. Moreover, when visualizing effects across all electrodes in all patients, we additionally corrected for multiple comparisons over electrodes, using FDR correction. All reported *P*-values are corrected and referred to as  $P_{\text{corr}}$ .

Peak latencies were identified within time-frequency windows of statistical significance on the difference between standard and deviant trials. For sustained responses, effect latencies were estimated as the earliest significant differences between deviant and standard trials. In both cases, reported latencies are the average latency across all significant electrodes.

### Functional Connectivity Analysis

Connectivity analyses were performed using pairwise phase consistency (PPC—Vinck et al. 2010), which provides a method for measuring rhythmic synchronization, without being affected by the finite sample size bias, observed with classic tools, such as phase locking value (PLV—Lachaux et al. 1999). This issue is particularly relevant when

comparing global deviant and standard conditions, as the number of trials in these conditions is different. In each trial  $j$ , for each time point  $t$  and frequency  $f$ , the phase  $\varphi_j(t, f)$  of the signal was estimated, using wavelets, as presented earlier. Pairwise phase consistency  $\text{PPC}_{kl}$  between electrodes  $k$  and  $l$  is then computed across  $N$  trials as follows:

$$\text{PPC}_{kl}(t) = \frac{2}{N(N-1)} \sum_{i=1}^{N-1} \sum_{j=i+1}^N \cos(\Delta\varphi_{kl}^i(t) - \Delta\varphi_{kl}^j(t)),$$

with  $\Delta\varphi_{kl}^i(t)$  the phase difference between electrodes  $k$  and  $l$  in trial  $i$  at time  $t$ .

Pairwise phase consistency was computed for all pairs of electrodes, for frequencies between 5 and 60 Hz, between 800 and 700 ms relative to the onset of the fifth sound. No baseline correction was applied.

Statistical significance was assessed by a nonparametric test on the difference of PPC between conditions (Lachaux et al. 1999), using 500 permutations, for each time and frequency samples, and cluster-based correction for multiple comparisons across time and frequency samples was applied (Maris and Oostenveld 2007). All reported  $P$ -values are corrected and referred to as  $P_{\text{corr}}$ . Given the high level of correlations between pairs of electrodes and the relatively low number of highly computationally demanding permutations, multiple comparisons are corrected only across time and frequency samples, but not across pairs of electrodes in order to avoid missing potentially relevant changes in functional connectivity (type II errors). However, this less conservative threshold could lead to false-positives (type I errors). This is why we report the average PPC changes across all pairs of temporal and frontal electrodes (see Fig. 4b).

The estimation of connectivity is based on the consistency of phase lags between areas. Note that consistent phase lags reflect the true connectivity between areas but also artifactual connectivity driven by synchronization of different areas onto any external reference. Therefore, we tried to isolate genuine synchronization between electrodes from spurious connectivity related to simultaneous processing of the stimuli (e.g. in left and right auditory cortices). We reasoned that spurious connectivity would be linked to oscillations evoked by the stimulations at several electrodes, as opposed to the induced activity that is time-locked, but not phase-locked, to the stimulation. We introduced a novel analysis, the induced PPC, based on the “evoked” versus “induced” terminology introduced by Tallon-Baudry and Bertrand (1999). For this analysis, the evoked oscillations were regressed out of the data and connectivity was estimated using the phase of the induced oscillations isolated in this way. Thus, induced PPC measures functional connectivity, which is not related to external stimulations. To compute this measure, we first averaged the data across trials in a given condition. This average preserves evoked oscillations and cancels out induced oscillations (Tallon-Baudry and Bertrand 1999). We then computed the time-frequency decomposition of this average using wavelets as described earlier. To isolate the induced response, we decompose data into time and frequency and regressed out linearly from each trial of a given condition the time-frequency decomposition of the corresponding evoked response. This corrected signal was used to compute the  $\text{PPC}_{\text{induced}}$ , and statistical comparisons were performed as previously described for the PPC.

## Results

Auditory novelty detection was studied using 282 intracranial electrodes across 9 epileptic patients, with an average of 31 (SD = 13) electrodes per patient (Table 1). Activity was recorded from the temporal lobe (194 electrodes), the frontal lobe (61 electrodes), and the occipital lobe (27 electrodes). Note that, as we did not have precise hypotheses about the laterality of the effects, we analyze electrodes from the left and right hemispheres together. All these patients performed the task properly (accuracy of >80%). We analyzed ERPs, time-frequency decompositions, and functional connectivity associated with local and global auditory novelty detection. This approach allowed us to test whether local novelty was related to an automatic and

encapsulated process and whether global novelty implicated distinct inter-connected brain regions.

## ERP Analysis

Significant responses to violation of local regularity (local deviant compared with local standard trials) were observed in 44 electrodes (16% of all the electrodes,  $t$ -test, all  $P_{\text{corr}} < 0.05$ ), all located in the temporal lobe. These responses were observed in 6 of the 8 patients with temporal electrodes. Notably, 20 of the 26 electrodes implanted in the superior temporal lobe (77%) showed significant local effect (Fig. 2a). The responses to local novelty presented 2 main components: an early one, with a peak on average at 133 ms (SD = 17 ms—see Fig. 2b for an exemplar electrode in which this peak is at 105 ms) after the onset of the fifth sound, and a second component, with a reversed polarity, showing a peak on average at 231 ms (SD = 33 ms—see Fig. 2b for an exemplar electrode in which this peak is at 165 ms). This local effect is related to the MMN observed in scalp EEG (Näätänen et al. 2001) and was found in previous intracranial studies (Halgren et al. 1995; Edwards et al. 2005; Bekinschtein et al. 2009). Note that, interestingly, the polarity of this component depends on the position of the electrode relative to the Sylvian fissure (Halgren et al. 1995). Moreover, in 8 of these 44 electrodes, from 3 different patients, these components were preceded by an event peaking on average at 71 ms (SD = 8 ms—see Fig. 2b for exemplar electrode in which this peak is at 63 ms) and which can be related to early components of novelty detection found in scalp EEG (Grimm et al. 2011). Finally, in 18 electrodes from 4 patients, the 2 main components were followed by an event with a peak on average at 435 ms (SD = 95 ms—see Fig. 2b for exemplar electrode in which this peak is at 330 ms), which may be related to the P3a (Halgren et al. 1995).

In contrast, responses to violation of global regularity (global deviant compared with global standard trials) were observed in 32 electrodes (11% of all the electrodes). These responses were more widespread across cortical structures than the local effect and were observed in 7 out of 9 patients. Twenty-four electrodes in the temporal lobe (24% of temporal electrodes), including 12 in the superior temporal lobe (46% of superior temporal lobe electrodes) and 8 in the frontal lobe (13% of frontal electrodes) showed significant effects ( $t$ -test, all  $P_{\text{corr}} < 0.05$ —Fig. 2a). The global effect was associated with 3 distinct components. First, in 19 electrodes from 5 patients, we observed a transient difference between global deviant and global standard trials on average at 226 ms (SD = 56 ms—see Fig. 2c for an exemplar electrode in which this component peaks at 260 ms), similar to the second component observed in response to local novelty. Indeed, only temporal electrodes showing this local effect presented such an early global effect. This component could be explained by a contextual modulation of the MMN amplitude. Indeed, local deviant stimuli are used in our paradigm both as global standards and as global deviants (Fig. 1). Thus, the probability of local deviant stimuli is not the same in each block, and this could affect the amplitude of the MMN (Sato et al. 2000; Wangcong et al. 2011; King et al. 2013). Second, a sustained difference starting on average at 366 ms (SD = 131 ms—see Fig. 2c for an exemplar electrode in which this component starts at 462 ms) was observed in response to global novelty in 20 electrodes from 7 patients. It has been associated with the P3b response observed in scalp EEG (Bekinschtein et al. 2009) and has been reported in previous intracranial studies (Smith et al. 1990;

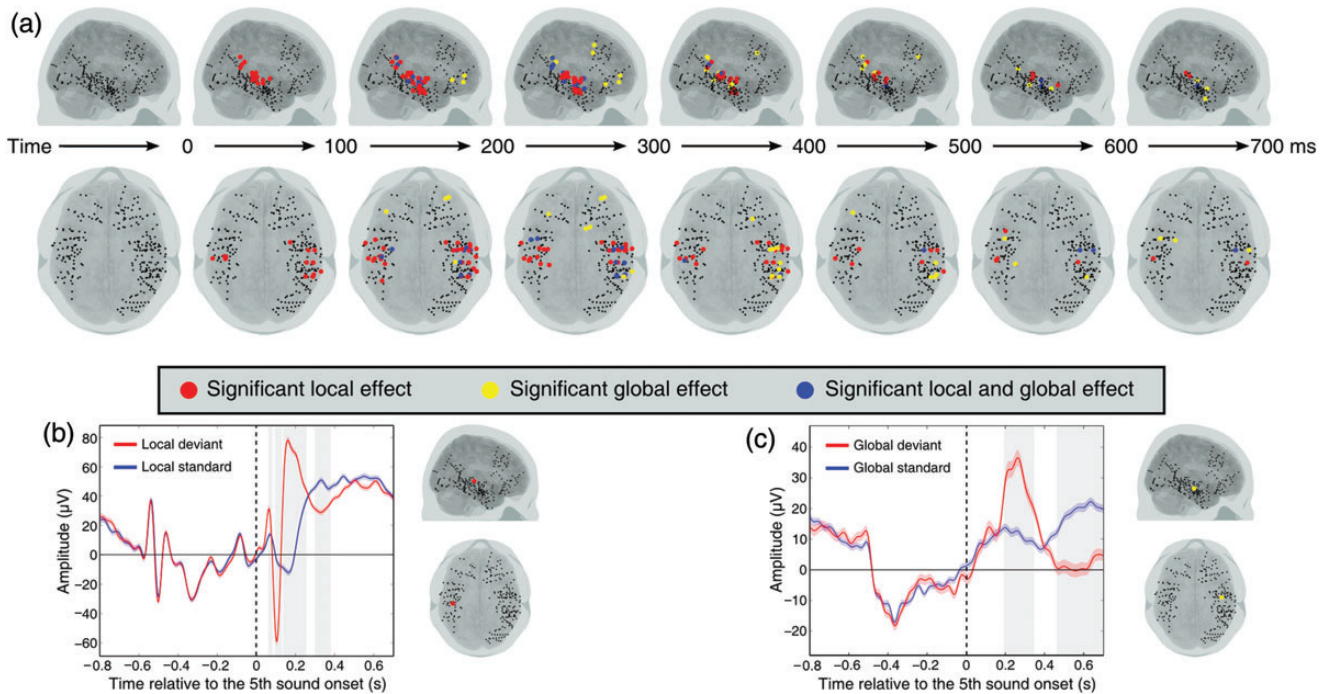


**Figure 2.** Event-related potentials in response to local and global novelty. (a) Localization of significant differences between standard and deviant stimuli. Each black dot represents an electrode. Red, yellow, and blue dots represent electrodes showing a significant local, global, and both local and global effect, respectively, in the time window indicated at the extremities of the black arrows. (b) Example of a temporal electrode showing significant differences between local deviant (in red) and local standard (in blue) stimuli. Four components, peaking at 63, 105, 165, and 330 ms, can be identified. Red and blue shadings represent SEM. Gray shading represents significant differences between conditions ( $P_{\text{corr}} < 0.05$ ). The precise localization of this electrode is shown on the right. (c) Example of a temporal electrode showing differences between global deviant (in red) and global standard (in blue) stimuli. Two components can be identified: the first one shows a peak at 260 ms, and the second one starts at 462 ms. Red and blue shadings represent SEM. Gray shading represents significant differences between conditions ( $P_{\text{corr}} < 0.05$ ). The precise localization of this electrode is shown on the right.

Baudena et al. 1995; Halgren et al. 1998). Note that the polarity of this component depends on the localization relative to the different generators (Smith et al. 1990). Finally, 2 electrodes from 1 patient implanted in the anterior cingulate cortex showed a transient response, with a peak on average at 265 ms but did not show any significant local effect. Note that we did not observe significant local or global effect in the occipital lobe. This may partly be explained by the low number of electrodes implanted in this region (only 27 electrodes, among which 25 belong to the same patient).

Note that the choice of the baseline time window could potentially influence the results, especially for the global effect as expectation-related components can build up (Faugeras et al. 2012). However, the number of electrodes showing significant local and global effects was not different when choosing a baseline expanding across the whole trial (for local effect:  $\chi^2 = 0.12$ ,  $P = 0.73$ ; for global effect:  $\chi^2 = 0.69$ ,  $P = 0.41$ ). We thus identified different ERP responses to local and global novelty. Local novelty was mainly associated with an early response restricted to the temporal local. In contrast, global novelty was associated with late responses in different brain regions.

### Time-Frequency Analysis

Task-induced activity was then analyzed in the time-frequency domain, using Morlet's wavelets. Violation of local regularity induced an increase in power in the gamma band (60–120 Hz) peaking on average 135 ms (SD = 45 ms) after the onset of the fifth sound, as revealed by the analysis of the proportion of

electrodes showing a significant effect ( $P_{\text{corr}} < 0.05$ ) at each time-frequency bin (Fig. 3a for exemplar electrode and Fig. 3b). This effect was observed in 22 electrodes (8% of all the electrodes), mostly implanted in the temporal lobe, in 6 out of the 9 patients. Among these electrodes, 9 were located in the superior temporal lobe (35% of superior temporal electrodes—Fig. 3c). One frontal electrode showed a similar effect (2% of frontal electrodes).

Violation of global regularity gave rise to an early increase in the gamma band peaking at 182 ms (SD = 50 ms). This modulation in the gamma band was similar to the one observed in the local effect, but more sustained in time. The increase in gamma power was observed in 6 of 9 patients, in 23 electrodes (8% of all the electrodes), mostly implanted in the temporal lobe as in the local effect, but it was also present in 5 frontal electrodes (8% of frontal electrodes), which, as reported previously, did not show a significant local effect (Fig. 3c). This first effect was followed by a decrease in the beta band (13–25 Hz), which started on average 258 ms (SD = 115 ms) after the fifth sound onset and was maintained until the end of the trial (Fig. 3a for exemplar electrodes and Fig. 3b). This decrease in beta-band power was observed in 26 electrodes (9% of all the electrodes) from 6 out of 9 patients and was widespread, affecting temporal but also 4 frontal electrodes (6% of frontal electrodes—see Fig. 3c). Similar to the ERP results, this beta-band response, which was sustained over time, was only observed in response to global novelty.

Interestingly, 16 of the 22 electrodes showing an increase in gamma band power in response to local novelty are also among the 44 electrodes showing a significant local ERP effect.

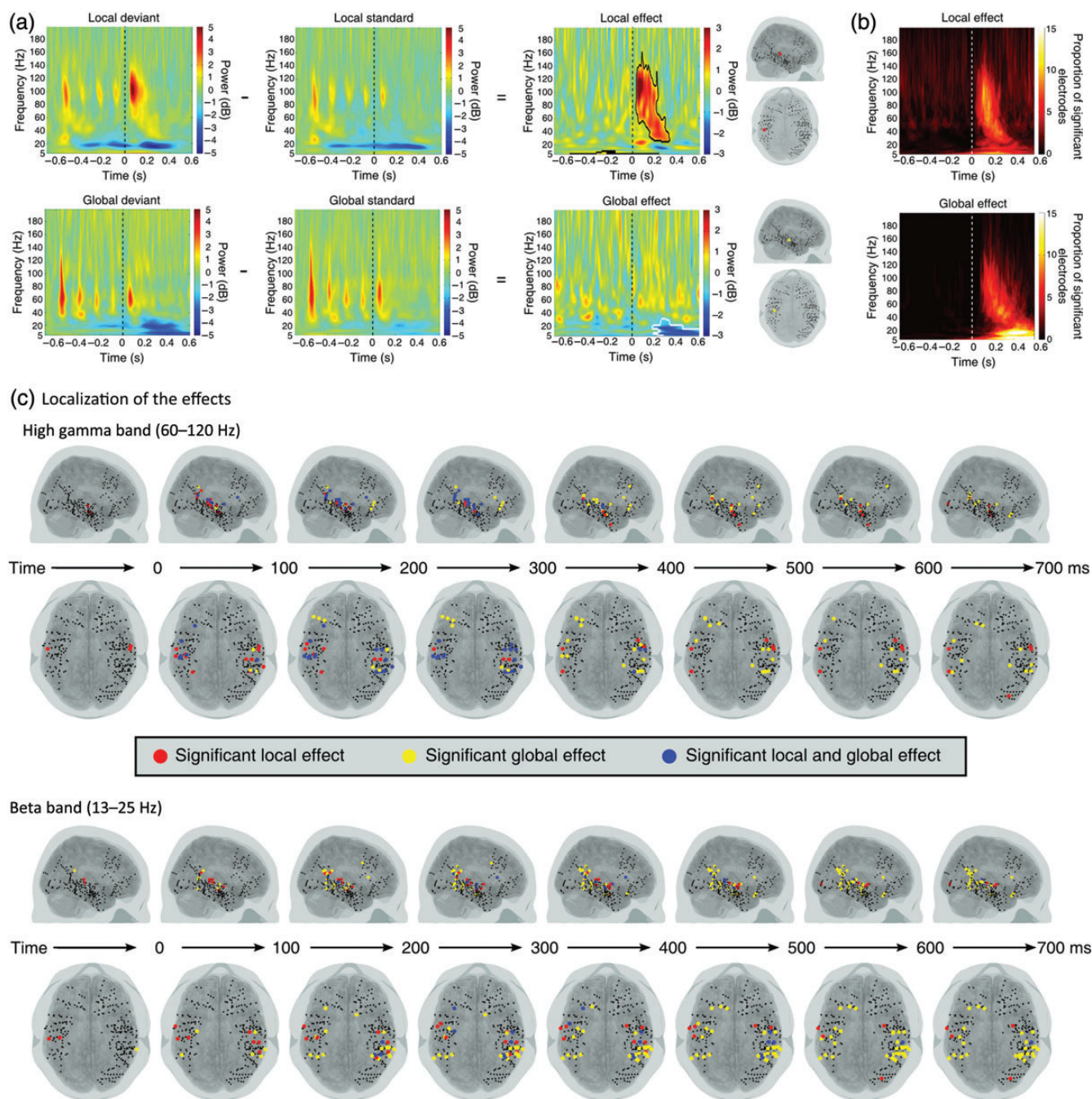


**Figure 3.** Time-frequency analysis. (a) Example of electrodes showing significant local and global effect. Top row, time-frequency responses of a temporal electrode to local deviant (left), local standard (middle), and local effect (difference between local deviant and local standard—right). Bottom row, time-frequency response of a temporal electrode to global deviant (left), global standard (middle), and global effect (difference between global deviant and global standard—right). Black and white contours circle significant time-frequency samples ( $P_{corr} < 0.05$ ). The precise localization of these electrodes is shown on far right. (b) Proportion of significant electrodes ( $P_{corr} < 0.05$ ) in each time and frequency bin for the local effect (top) and the global effect (bottom). (c) Localization of significant effects in the high gamma band (top) and the beta band (bottom). Each black dot represents an electrode. Red, yellow, and blue dots represent electrodes showing significant local, global, and both local and global effects, respectively, in the time window indicated at the extremities of the black arrows.

Note that the latency of the gamma band response is very similar to that of the early response to local novelty observed in ERP. Moreover, 15 of the 23 electrodes showing an increase in gamma band power in response to global novelty are also among the 32 electrodes showing a significant ERP response to global novelty. Finally, only 7 electrodes belonged both to the set of 32 electrodes showing a significant ERP response to global novelty and to the set of 26 electrodes showing a

decrease in the beta band in response to global novelty. These results highlight the fact that ERP and time-frequency analyses extract different facets of the responses to local and global novelty, as significant effects identified with both methods are not necessarily present in the same electrodes.

Local and global novelties were associated with different time-frequency responses. Violations of local regularity were related to an early increase in high gamma power. In contrast,

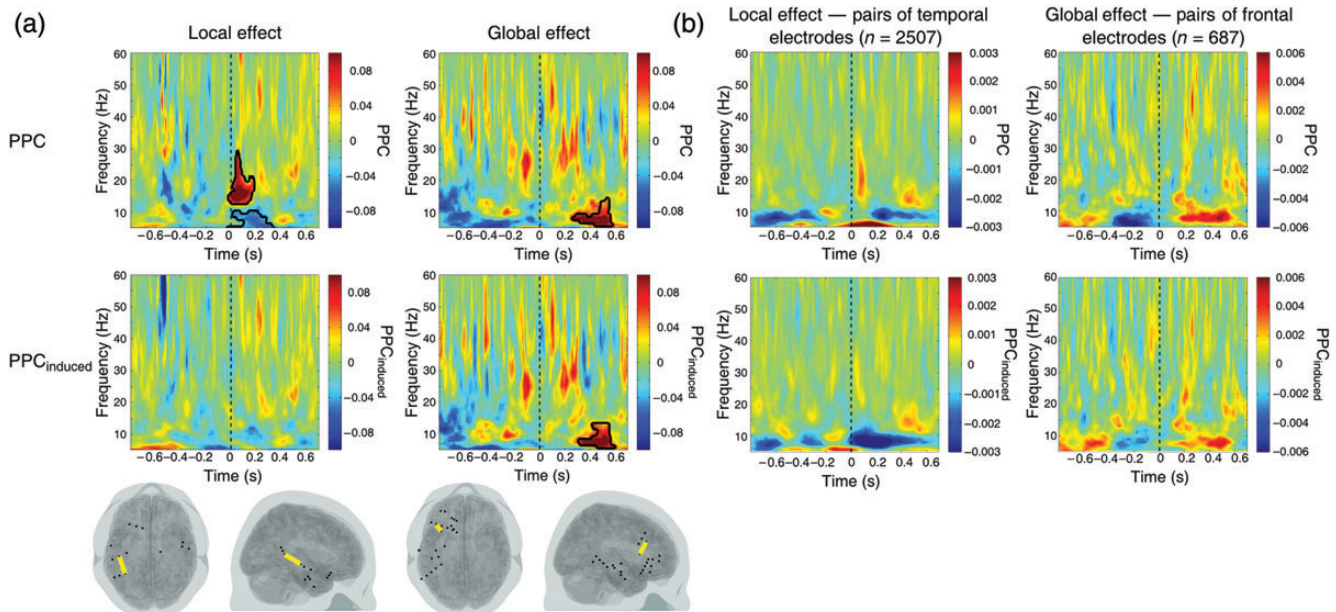


**Figure 4.** Functional connectivity. (a) Time-frequency representations of pairwise phase consistency (PPC—top row) and induced PPC (middle row) modulations in 2 pairs of electrodes. On the left, differences in PPC and induced PPC between local deviant and local standard stimuli in a pair of temporal electrodes are represented. On the right, differences in PPC and induced PPC between global deviant and global standard stimuli in a pair of frontal electrodes are represented. The bottom row shows the localization of these pairs. Black contours circle significant time-frequency samples ( $P_{\text{corr}} < 0.05$ ). (b) On the left, average differences in PPC (top) and induced PPC (bottom) between local standard and local deviant stimuli in pairs of temporal electrodes ( $n = 2507$ ) are presented. On the right, average differences in PPC (top) and induced PPC (bottom) between global standard and global deviant stimuli in pairs of frontal electrodes ( $n = 687$ ) are presented.

violations of global regularity were associated with a sustained decrease in beta power. Interestingly, these time-frequency responses highlight different aspects of brain responses to local and global novelty than ERP responses.

### Functional Connectivity Analysis

Changes in connectivity related to the task were analyzed using PPC, a measure of synchronization that is not biased by the number of trials in each condition (Vinck et al. 2010). We report results for all pairs of electrodes ( $n = 4714$ ) to identify modulation of connectivity in response to local and global novelty, with a special focus on the temporal and frontal lobes, as most of the electrodes were implanted in these regions and no significant response was observed in the other lobes in ERP and time-frequency analyses. There were 2507 pairs between temporal electrodes, 687 pairs between frontal electrodes, 539 pairs between temporal and frontal electrodes, 301 pairs between occipital electrodes, and 680 pairs between occipital and temporal electrodes.

Local novelty was associated with a transient increase in functional connectivity, as measured by PPC, in the beta band (13–25 Hz), centered at 80 ms after the onset of the fifth sound (see Fig. 4a for exemplar pair). This increase was significant ( $P_{\text{corr}} < 0.05$ ) in 38 pairs of electrodes (1% of all the electrode pairs), in 7 of 9 patients. All of these pairs, but 5, were between temporal electrodes (see Fig. 4b for the average across all pairs of temporal electrodes). Interestingly, only 9 of them showed a similar increase in the PPC-induced analysis. This suggests that the effect is related to activity evoked by the stimuli and can be partly explained by a parallel and simultaneous processing of the sounds rather than by a genuine inter-area exchange of information. Local novelty was also associated with a decrease in PPC in the beta band in 20 other pairs of temporal electrodes.

Among them, 18 pairs showed a similar decrease in induced PPC.

On the other hand, global novelty was associated with a sustained increase in PPC in the alpha band (8–13 Hz), starting at 160 ms after the onset of the fifth sound and lasting until 600 ms after the onset of the fifth sound (see Fig. 4a for exemplar pair and Fig. 4b). This effect was observed in 7 of 9 patients in 49 pairs of electrodes (1% of all electrode pairs): 27 between temporal electrodes (1% of temporal pairs), 7 between frontal electrodes (1% of frontal pairs), 5 between frontal and temporal electrodes (1% of temporo-frontal pairs), and 10 between occipital and temporal electrodes (1% of occipito-temporal pairs). Interestingly, among these electrode pairs, 42 showed this late increase in connectivity in the PPC-induced analysis, which suggests that it is related to a genuine synchronization, and not simply to a simultaneous processing of the stimuli. Global novelty was also associated with a sustained decrease in PPC in 100 pairs of electrodes, in the same time window as the increase described earlier. This decrease was also observed in these pairs in the PPC-induced analysis. Among these pairs, 66 were between temporal electrodes, 28 between occipital and temporal electrodes, 1 between temporal and frontal electrodes, 5 between occipital electrodes, and 1 between frontal electrodes. Note, however, that this decrease in connectivity was mainly observed in Patient 9, for whom 78 significant pairs were observed. This patient was the only one with occipital and posterior temporal electrodes.

Interestingly, the increase in PPC in response to local novelty implicated 45 electrodes, among which 16 also showed an ERP effect and 11 showed a time-frequency response to local novelty. The increase in PPC-induced in response to local novelty implicated 19 of these 45 electrodes, among which 7 showed an ERP effect and 5 showed an increase in

gamma power in response to local novelty. In response to global novelty, the increase in PPC implicated 67 electrodes, among which 9 showed an ERP effect and 16 showed a time-frequency response to global novelty. Only 6 of these 67 electrodes were not in pairs of electrodes showing an increase in PPC<sub>induced</sub> in response to global novelty. Among these 6 electrodes, 3 showed a significant ERP response and 2 showed a time-frequency response to global novelty.

Local novelty was thus associated with an early increase in functional connectivity in the beta band, mostly in pairs of temporal electrodes. This increase was not present in most of these pairs in the PPC<sub>induced</sub> analysis, so it may probably partly explained by the simultaneous processing of the stimuli by different brain regions. In contrast, global novelty was associated with a late increase in alpha-band functional connectivity. This increase was observed even when using PPC<sub>induced</sub>, suggesting that this increase is related to genuine synchronization between brain areas.

## Discussion

We studied the responses to 2 embedded levels of auditory novelty, defined at local (within trials) and global (between trials) scales, in 9 epileptic patients implanted with 282 depth electrodes. We report for the first time a systematic description of processes underlying local and global novelty detection combining ERPs, time-frequency, and functional connectivity measures. These 3 facets converged to delineate several differences between these 2 neural events, supporting the hypotheses that the local novelty detection is associated with an early process confined to the temporal lobe, whereas in contrast, global novelty detection is processed later and implies the coordinated activity of distributed brain regions interacting together in the slow frequency range.

### Two Distinct Neural Events

Detection of local novelty was reflected in 2 successive ERP components (peaking on average at 133 and 231 ms). This intracranial ERP response has previously been associated with the MMN observed in scalp EEG in response to local novelty, as it is observed in brain regions identified by source reconstruction of the MMN, and it has a similar time course (Bekinschtein et al. 2009). It also has been reported in previous intracranial studies (Halgren et al. 1995; Liasis et al. 2001; Edwards et al. 2005; Rosburg et al. 2005). Detection of local novelty was also reflected in a transient increase in high gamma (60–120 Hz) activity, peaking on average at 135 ms after the onset of the critical sound, and an increase in local connectivity, as measured by PPC, in the beta band (13–25 Hz). This increase was centered on average around 80 ms after the onset of the critical sound and was observed only in pairs of temporal electrodes. Interestingly, this change in connectivity could not be measured by the induced PPC in most of these pairs of electrodes, which suggests that it can be partially explained by a simultaneous and parallel processing of the stimuli in different recording sites (e.g. in the auditory cortex of both hemispheres). Importantly, those 3 responses were exclusively observed within the temporal lobe, and more precisely in the superior temporal plane.

On the contrary, responses to global novelty were distributed in multiple cortical areas, and in particular in temporal and frontal regions. They comprised a sustained ERP difference

starting on average 366 ms after the onset of the fifth sound. This ERP response has been associated with the P3b response observed in scalp EEG in response to global novelty, as it is observed in regions identified as sources of the P3b (Bekinschtein et al. 2009). It has also been reported in previous intracranial studies (Smith et al. 1990; Baudena et al. 1995; Halgren et al. 1998). Moreover, responses to global novelty also included a sustained decrease in beta (13–25 Hz) power starting on average 258 ms after the onset of the critical sound and a prolonged increase in PPC in the alpha band (8–12 Hz) beginning from 160 ms after the onset of the fifth sound, particularly in pairs of frontal electrodes. A similar effect was observed with the induced PPC, which suggests genuine changes in functional connectivity in this time window, over and above the mere propagation of stimulus-induced activation. These results need to be confirmed in future studies, as the high dependency between pairs of electrodes did not allow us to correct for multiple comparison across pairs of electrodes, but only across time and frequency samples. Moreover, as for all intracranial EEG studies, estimation of network connectivity was limited by the localization of recording sites in each patient. Notably, it would have been interesting to refine our understanding of the interactions between temporal and frontal electrodes, but only 3 patients presented recording sites in both of these regions.

### Local Processing versus Long-Range Interactions

Our time-frequency results revealed opposite patterns of spectral power for local and global novelties. Local novelty elicited an early and transient increase in high gamma (60–120 Hz) power within the auditory cortex, in agreement with a previous intracranial study using a classical oddball paradigm (Edwards et al. 2005). Conversely, a distributed, late, and sustained decrease in power in the beta (13–25 Hz) band was observed in response to global novelty. Interestingly, high gamma activity has been proposed as a signature of local spiking activity (Pesaran et al. 2002; Nir et al. 2007; Ray and Maunsell 2010), whereas modulations of power in the beta band are thought to reflect long-range interactions (Kopell et al. 2000). Moreover, a recent framework (Donner and Siegel 2011) associates high gamma activity with encoding functions and lower frequency (including beta band) oscillations with integrative functions. Our results are in agreement with this framework, as the global effect involves the integration of sounds over several trials to identify the relevant rule, whereas the local effect reflects the encoding of changes in basic features of the sound. Note, however, that the PPC analysis did not allow us to identify long-range interactions in response to global novelty. This may be related to the few long-range pairs of electrodes present in this dataset, as for example only 3 patients were implanted both in the temporal and the frontal lobes.

### Partition of the MMN into 2 Successive Events

Our observation of 2 successive events in our ERP analysis of responses to local novelty supports the partition of the MMN in 2 main components: 1) an early automatic, non-conscious, and short-lived echoic memory system located within the auditory cortex, termed “early MMN” (Pegado et al. 2010) and 2) a later response extending beyond early auditory areas, and showing a stronger resistance to increases in the temporal spacing of sounds, corresponding to the N2b component or “late MMN”

(Pegado et al. 2010). These results are in agreement with previous intracranial studies using a classical oddball paradigm (Halgren et al. 1995). Interestingly, the N2b has been associated with attention (Näätänen and Gaillard 1983), contrary to the “early MMN,” which is thought to reflect automatic processing of novelty. In Pegado et al.’s (2010), the authors show that when increasing the SOA between 2 successive sounds beyond 1000 ms in a traditional oddball paradigm, the disappearance of the “early MMN” actually corresponds to the occurrence of a similar novelty response present both for deviant and standard trials. In contrast, the “late MMN” latency was delayed, but this component did not disappear. Pegado et al. proposed a model accounting for these results: the early MMN would reflect accumulation of evidence based on echoic memory representations, whereas the late MMN would be related to accumulation of evidence on longer time scales. In our study, the early MMN would thus be absent in the global novelty condition because the relevant time scales are longer than in the local novelty condition. Conversely, given the resistance of the “late MMN” to SOA, it would not be surprising to observe its presence in response to global novelty.

In the present study, no MMN was recorded in frontal electrodes, in agreement with some previous intracranial studies (Baudena et al. 1995; Edwards et al. 2005). Nevertheless, because of the non-uniform sampling of our recording sites over the frontal lobe, it cannot be excluded that a frontal generator of the MMN exists but was missed, as suggested by some scalp EEG studies (Giard et al. 1990; Rinne et al. 2000; Opitz et al. 2002). Note that in a study including only 2 implanted patients (Bekinschtein et al. 2009), using less conservative statistical thresholds, we previously reported 3 frontal electrodes with a local effect, in agreement with other intracranial studies (Liasis et al. 2001; Rosburg et al. 2005).

### Global Effect and Conscious Access

The paradigm used in this study was designed to dissociate 2 different processes, underlying local and global novelty detection. In a previous experiment using this paradigm, we showed that while the response to local novelty was still observed under conditions of inattention (engagement in a concurrent difficult RSVP task), the response to global novelty disappeared and subjects could not report the existence of violations of the global regularity in EEG and MEG studies (Bekinschtein et al. 2009). Moreover, this paradigm was used in patients suffering from disorders of consciousness, and the response to global novelty was only observed in patients showing signs of consciousness (Bekinschtein et al. 2009; Fugeras et al. 2011, 2012; King et al. 2013). The P3b component has also been proposed as a marker of conscious access in other paradigms (Sergent et al. 2005). Note, however, that in the present study, patients were instructed to count global deviant trials. The responses to global novelty could thus reflect downstream processes relative to conscious access *per se* (Aru et al. 2012; Sergent and Naccache 2012).

To distinguish between these “downstream” processes and signatures of conscious access, it is interesting to compare our results with studies using a different task. First, Wacongne et al. (2011) used a passive version of the Local/Global paradigm and found similar ERP signatures of local and global novelty. Moreover, in a completely different study contrasting masked and unmasked words, Gaillard et al. (2009) explored ERPs, time-frequency changes, and connectivity patterns in

intracranial EEG—similarly to the approach taken in the present study—and reported closely related findings. Conscious processing of unmasked words was associated with sustained event-related components, notably in the frontal cortex, a decrease in power in the beta band and a late increase in connectivity in the alpha and beta band. The single discrepancy with our findings is the small proportion of electrodes in which we observed the 3 signatures of the late global effect. This could be explained by the fact that the global effect corresponds to a more subtle contrast than the masked/unmasked contrast. Indeed, whereas the masked/unmasked contrast compared a “no stimulus” condition with a “stimulus present” condition, we contrasted here 2 conditions associated with conscious perception: global deviant stimuli being perceived as violations of the global regularity, and global standard stimuli as regular trials.

Nevertheless, we conclude by highlighting the striking similarity between our results and the 3 signatures of conscious perception identified by Gaillard et al, despite the profound difference in sensory modalities (audition versus vision), in stimuli (words versus tones) and tasks. This may point to a general common mechanism of conscious access (Sergent and Naccache 2012).

### Funding

This work was supported by the program “Investissements d’avenir” ANR-10-IAIHU-06, an AXA Research Fund grant to IEK, a Direction Générale de l’Armement (DGA) grant to JRK, a Ministère de l’Enseignement Supérieur et de la Recherche grant to FM, a Rubicon grant from the Netherlands Organization for Scientific Research (NWO) to SvG, an “Equipe FRM 2010” grant of Fondation pour la Recherche Médicale (FRM) to LN and an European Research Council (ERC) senior grant “NeuroConsc” to SD.

### Notes

We thank Séverine Samson and Isabelle Jegourel for their help in gathering clinical information and all the patients for their time and kindness. *Conflict of Interest:* None declared.

### References

- Aru J, Bachmann T, Singer W, Melloni L. 2012. Distilling the neural correlates of consciousness. *Neurosci Biobehav Rev.* 36:737–746.
- Atienza M, Cantero JL, Gómez CM. 1997. The mismatch negativity component reveals the sensory memory during REM sleep in humans. *Neurosci Lett.* 237:21–24.
- Axmacher N, Cohen MX, Fell J, Haupt S, Dümpelmann M, Elger CE, Schlaepfer TE, Lenartz D, Sturm V, Ranganath C. 2010. Intracranial EEG correlates of expectancy and memory formation in the human hippocampus and nucleus accumbens. *Neuron.* 65:541–549.
- Baudena P, Halgren E, Heit G, Clarke JM. 1995. Intracerebral potentials to rare target and distractor auditory and visual stimuli. III. Frontal cortex. *Electroencephalogr Clin Neurophysiol.* 94:251–264.
- Bekinschtein TA, Dehaene S, Rohaut B, Tadel F, Cohen L, Naccache L. 2009. Neural signature of the conscious processing of auditory regularities. *Proc Natl Acad Sci USA.* 106:1672–1677.
- De Moortel I, Munday SA, Hood AW. 2004. Wavelet analysis: the effect of varying basic wavelet parameters. *Sol Phys.* 222:203–228.
- Donchin E, Coles MGH. 1988. Is the P300 component a manifestation of context updating? *Behav Brain Sci.* 11:357–374.
- Donner TH, Siegel M. 2011. A framework for local cortical oscillation patterns. *Trends Cogn Sci.* 15:191–199.

- Edwards E, Soltani M, Deouell LY, Berger MS, Knight RT. 2005. High gamma activity in response to deviant auditory stimuli recorded directly from human cortex. *J Neurophysiol*. 94:4269–4280.
- Fang Q. 2010. Mesh-based Monte Carlo method using fast ray-tracing in Plücker coordinates. *Biomed Opt Express*. 1:165–175.
- Fang Q, Boas DA. 2009. Tetrahedral mesh generation from volumetric binary and grayscale images. *Proceedings of IEEE Int Symp Biomed Imaging 2009*. 2009 June 28–July 1. Boston, MA: IEEE. p. 1142–1145.
- Faugeras F, Rohaut B, Weiss N, Bekinschtein T, Galanaud D, Puybasset L, Bolgert F, Sergent C, Cohen L, Dehaene S et al. 2012. Event related potentials elicited by violations of auditory regularities in patients with impaired consciousness. *Neuropsychologia*. 50:403–418.
- Faugeras F, Rohaut B, Weiss N, Bekinschtein TA, Galanaud D, Puybasset L, Bolgert F, Sergent C, Cohen L, Dehaene S et al. 2011. Probing consciousness with event-related potentials in the vegetative state. *Neurology*. 77:264–268.
- Fischer C, Morlet D, Bouchet P, Luaute J, Jourdan C, Salord F. 1999. Mismatch negativity and late auditory evoked potentials in comatose patients. *Clin Neurophysiol*. 110:1601–1610.
- Fries P. 2005. A mechanism for cognitive dynamics: neuronal communication through neuronal coherence. *Trends Cogn Sci*. 9:474–480.
- Gaillard R, Dehaene S, Adam C, Clémenceau S, Hasboun D, Baulac M, Cohen L, Naccache L. 2009. Converging intracranial markers of conscious access. *PLoS Biol*. 7:e1000061.
- Giard M-H, Perrin F, Pernier J, Bouchet P. 1990. Brain generators implicated in the processing of auditory stimulus deviance: a topographic event-related potential study. *Psychophysiology*. 27:627–640.
- Grimm S, Escera C, Slabu L, Costa-Faidella J. 2011. Electrophysiological evidence for the hierarchical organization of auditory change detection in the human brain. *Psychophysiology*. 48:377–384.
- Halgren E, Baudena P, Clarke JM, Heit G, Liégeois C, Chauvel P, Musolino A. 1995. Intracerebral potentials to rare target and distractor auditory and visual stimuli. I. Superior temporal plane and parietal lobe. *Electroencephalogr Clin Neurophysiol*. 94:191–220.
- Halgren E, Baudena P, Clarke JM, Heit G, Marinkovic K, Devaux B, Vignal J-P, Biraben A. 1995. Intracerebral potentials to rare target and distractor auditory and visual stimuli. II. Medial, lateral and posterior temporal lobe. *Electroencephalogr Clin Neurophysiol*. 94:229–250.
- Halgren E, Marinkovic K, Chauvel P. 1998. Generators of the late cognitive potentials in auditory and visual oddball tasks. *Electroencephalogr Clin Neurophysiol*. 106:156–164.
- King JR, Faugeras F, Gramfort A, Schurger A, El Karoui I, Sitt JD, Rohaut B, Wacongne C, Labyt E, Bekinschtein T et al. 2013. Single-trial decoding of auditory novelty responses facilitates the detection of residual consciousness. *Neuroimage*. 83:726–738.
- Kopell NJ, Ermentrout GB, Whittington M, Traub RD. 2000. Gamma rhythms and beta rhythms have different synchronization properties. *Proc Natl Acad Sci USA*. 97:1867–1872.
- Kropotov JD, Alho K, Näätänen R, Ponomarev VA, Kropotova OV, Anichkov AD, Nechaev VB. 2000. Human auditory-cortex mechanisms of preattentive sound discrimination. *Neurosci Lett*. 280:87–90.
- Lachaux J-P, Rodriguez E, Martinerie J, Varela FJ. 1999. Measuring Phase Synchrony in Brain Signals. *Hum Brain Mapp*. 8:194–208.
- Liasis A, Towell A, Alho K, Boyd S. 2001. Intracranial identification of an electric frontal-cortex response to auditory stimulus change: a case study. *Brain Res Cogn Brain Res*. 11:227–233.
- Maris E, Oostenveld R. 2007. Nonparametric statistical testing of EEG- and MEG-data. *J Neurosci Methods*. 164:177–190.
- Näätänen R, Gaillard AWK. 1983. The orienting reflex and the N2 deflection of the event-related potentials. In: *Tutorials in event related potential research: endogenous components*. *Advances in Psychology*. Elsevier. p. 119–141.
- Näätänen R, Gaillard AWK, Mäntysalo S. 1978. Early selective-attention effect on evoked potential reinterpreted. *Acta Psychol (Amst)*. 42:313–329.
- Näätänen R, Tervaniemi M, Sussman E, Paavilainen P, Winkler I. 2001. “Primitive intelligence” in the auditory cortex. *Trends Neurosci*. 24:283–288.
- Naccache L, Puybasset L, Gaillard R, Serve E, Willer J-C. 2005. Auditory mismatch negativity is a good predictor of awakening in comatose patients: a fast and reliable procedure. *Clin Neurophysiol*. 116:988–989.
- Nichols TE, Holmes AP. 2002. Nonparametric permutation tests for functional neuroimaging: a primer with examples. *Hum Brain Mapp*. 15:1–25.
- Nir Y, Fisch L, Mukamel R, Gelbard-Sagiv H, Arieli A, Fried I, Malach R. 2007. Coupling between neuronal firing rate, gamma LFP, and BOLD fMRI is related to interneuronal correlations. *Curr Biol*. 17:1275–1285.
- Oostenveld R, Fries P, Maris E, Schoffelen J-M. 2011. FieldTrip: open source software for advanced analysis of MEG, EEG, and invasive electrophysiological data. *Comput Intell Neurosci*. 2011:1–9.
- Opitz B, Rinne T, Mecklinger A, von Cramon DY, Schröger E. 2002. Differential contribution of frontal and temporal cortices to auditory change detection: fMRI and ERP results. *Neuroimage*. 15:167–174.
- Pegado F, Bekinschtein TA, Chausson N, Dehaene S, Cohen L, Naccache L. 2010. Probing the lifetimes of auditory novelty detection processes. *Neuropsychologia*. 48:3145–3154.
- Pesaran B, Pezaris JS, Sahani M, Mitra PP, Andersen RA. 2002. Temporal structure in neuronal activity during working memory in macaque parietal cortex. *Nat Neurosci*. 5:805–811.
- Pfurtscheller G, Lopes da Silva FH. 1999. Event-related EEG/MEG synchronization and desynchronization: basic principles. *Clin Neurophysiol*. 110:1842–1857.
- Picton TW. 1992. The P300 wave of the human event-related potential. *J Clin Neurophysiol*. 9:456–479.
- Polich J. 2007. Updating P300: an integrative theory of P3a and P3b. *Clin Neurophysiol*. 118:2128–2148.
- Ray S, Maunsell JHR. 2010. Differences in gamma frequencies across visual cortex restrict their possible use in computation. *Neuron*. 67:885–896.
- Rinne T, Alho K, Ilmoniemi RJ, Virtanen J, Näätänen R. 2000. Separate time behaviors of the temporal and frontal mismatch negativity sources. *Neuroimage*. 12:14–19.
- Rosburg T, Trautner P, Dietl T, Korzyukov OA, Boutros NN, Schaller C, Elger CE, Kurthen M. 2005. Subdural recordings of the mismatch negativity (MMN) in patients with focal epilepsy. *Brain*. 128:819–828.
- Sato Y, Yabe H, Hiruma T, Sutoh T, Shinozaki N, Nashida T, Kaneko S. 2000. The effect of deviant stimulus probability on the human mismatch process. *Neuroreport*. 11:3703–3708.
- Sergent C, Baillet S, Dehaene S. 2005. Timing of the brain events underlying access to consciousness during the attentional blink. *Nat Neurosci*. 8:1391–1400.
- Sergent C, Naccache L. 2012. Imaging neural signatures of consciousness: “what”, “when”, “where” and “how” does it work? *Arch Ital Biol*. 150:91–106.
- Smith ME, Halgren E, Sokolik M, Baudena P, Musolino A, Liégeois-Chauvel C, Chauvel P. 1990. The intracranial topography of the P3 event-related potential elicited during auditory oddball. *Electroencephalogr Clin Neurophysiol*. 76:235–248.
- Squires NK, Squires KC, Hillyard SA. 1975. Two varieties of long-latency positive waves evoked by unpredictable auditory stimuli in man. *Electroencephalogr Clin Neurophysiol*. 38:387–401.
- Sutton S, Braren M, Zubin J, John ER. 1965. Evoked-potential correlates of stimulus uncertainty. *Science*. 150:1187–1188.
- Tallon-Baudry C, Bertrand O. 1999. Oscillatory gamma activity in humans and its role in object representation. *Trends Cogn Sci*. 3:151–162.
- Tallon-Baudry C, Bertrand O, Delpuech C, Pernier J. 1997. Oscillatory gamma-band (30–70 Hz) activity induced by a visual search task in humans. *J Neurosci*. 17:722–734.
- Vinck M, van Wingerden M, Womelsdorf T, Fries P, Pennartz CMA. 2010. The pairwise phase consistency: a bias-free measure of rhythmic neuronal synchronization. *Neuroimage*. 51:112–122.
- Wacongne C, Labyt E, van Wassenhove V, Bekinschtein T, Naccache L, Dehaene S. 2011. Evidence for a hierarchy of predictions and prediction errors in human cortex. *Proc Natl Acad Sci USA*. 108:20754–20759.
- Zaehle T, Bauch EM, Hinrichs H, Schmitt FC, Voges J, Heinze H-J, Bunzeck N. 2013. Nucleus accumbens activity dissociates different forms of salience: evidence from human intracranial recordings. *J Neurosci*. 33:8764–8771.